



Water Oxidation by Manganese Oxide Electrocatalytic Films Synthesized by Chemical Solution Deposition Method

Hyo Sang Jeon,^{a,=} Su Jin Ahn,^{a,b,=} Michael Shincheon Jee,^a Sam S. Yoon,^{b,c}
Yun Jeong Hwang,^a and Byoung Koun Min^{a,b,z}

^aClean Energy Research Center, Korea Institute of Science and Technology, Seoul 02792, Korea

^bGreen School, Korea University, Seoul 02841, Korea

^cSchool of Mechanical Engineering, Korea University, Seoul 02841, Korea

Water splitting catalyzed by low cost and earth abundant material is critically important issue in mass production of hydrogen from water using electrical energy. In this study, we developed highly efficient manganese oxide (MnO_x) electrocatalytic films by a simple chemical solution deposition (CSD) method for oxygen evolution reaction (OER). Specifically, the MnO_x electrocatalytic films were synthesized at different annealing temperatures at 350, 450, and 550°C after the precursor solution coating on fluorine-doped tin oxide (FTO) glass substrates. The MnO_x electrocatalytic film prepared at 450°C has exhibited the most catalytic activity for OER with the overpotential of 387 mV at 10 mA/cm² in 1 M NaOH alkaline solution. We suggested that this high OER activity of MnO_x electrocatalytic film arise from the higher surface area, richer Mn³⁺ state on the catalysts surface, and low charge transfer resistance between electrocatalytic film and electrolyte based on electrochemical surface area (ECSA), X-ray photoelectron spectroscopy (XPS), and electrochemical impedance spectroscopy (EIS) analysis.

© 2016 The Electrochemical Society. [DOI: 10.1149/2.0171611jes] All rights reserved.

Manuscript submitted March 28, 2016; revised manuscript received June 13, 2016. Published July 20, 2016. *This paper is part of the JES Focus Issue on Electrolysis for Increased Renewable Energy Penetration.*

Oxygen evolution reaction (OER) is well known and important electrochemical process for water splitting and solar-fuel production technologies.¹⁻⁵ The challenge in this process is to diminish overpotential to overcome high activation energy barrier involving the complicated four electron process for the oxidation of water. Thus, electrocatalysts for OER is being developed to solve this issue. The photosystem II of photosynthesis in nature have manganese-based catalyst in the form of CaMn₄O₅ cluster for facilitating photosynthetic water oxidation which performs with an extremely low overpotential (~160 mV).^{6,7} Inspired from nature, many researchers have been focusing on the development of manganese-based catalysts which are earth abundant and inexpensive materials.

Among the various manganese-based materials, manganese oxide (MnO_x) is a widely reported catalyst for OER in an alkaline aqueous solution.⁸⁻¹² In particular, Mn₂O₃ has been suggested as an excellent OER catalysts over other phase of MnO_x such as MnO₂, Mn₃O₄ and MnOOH because it contains significant amounts of Mn³⁺ oxidation state which has been revealed to be the active site.¹³ Furthermore, it is possible to achieve better catalytic activities for OER than bulk catalysts by controlling the morphology of Mn₂O₃ catalysts. For example, Kuo et al. reported mesoporous Mn₂O₃ synthesized by a sol-gel process and exhibited highly active performance for OER with turnover frequency of $1.05 \times 10^{-3} \text{ s}^{-1}$ which is comparable to the most active RuO₂ ($3.87 \times 10^{-3} \text{ s}^{-1}$).¹⁴ However, in these studies, preparation processes for electrocatalytic film as an electrode were complicated and time-consuming because of the involvement of two separate steps: the catalysts is synthesized beforehand and is deposited onto a substrate usually with a binder material, which is often detrimental to the electrode function. Therefore, it is crucial to develop more simplified methods to prepare electrocatalytic films as electrodes.

Among the various methods to fabricate electrocatalytic films, chemical solution deposition (CSD) has been a suggested method for a simple formation of oxide materials onto a substrate.¹⁵ This method can be summarized in three steps: firstly, metal precursor was dissolved in a desired solvent to prepare a precursor solution; secondly, the solutions were deposited onto the substrate by using various coating methods such as spin coating and spray deposition; and lastly, films are thermally oxidized with heat-treatment to syn-

thesize a crystalline metal oxide. In particular, by using precursor solution with specific polymers as a soft template (e.g. ethylcellulose), it is possible to fabricate electrocatalytic films with porous structures with high surface area directly onto the substrate.¹⁶ Thus, CSD is an attractive method for the easily preparing an electrode; therefore, has already been applied in the diverse research areas (e.g. dye-sensitized solar cells, solution processed thin film solar cells, etc.).^{17,18}

In this study, we successfully synthesized MnO_x electrocatalytic films via CSD method which demonstrates the feasibility of low cost processing of an earth abundant material for OER. A precursor solution with manganese nitrate and ethylcellulose as a soft template was coated on fluorine doped tin oxide (FTO) glass substrates followed by annealing at various temperatures. We could confirm that OER activities depend on the annealing temperature, and the MnO_x electrocatalytic film annealed at 450°C exhibited the best OER activity with an overpotential of 387 mV at 10 mA/cm². The changes in the electrocatalytic film properties and its impact on the OER activities according to the annealing temperature was analyzed with electrochemical surface area (ECSA) measurements, X-ray photoelectron spectroscopy (XPS), and electrochemical impedance spectroscopy (EIS).

Experimental

Preparation of MnO_x electrocatalytic films by chemical solution deposition (CSD) method.—Mn(NO₃)₂ · xH₂O (Aldrich, 1.0 g) was dissolved in ethanol (5.0 mL) followed by adding an ethanol solution (10.0 mL) mixed with ethyl-cellulose (EC) (Aldrich, 0.5 g) and alpha-terpineol (Aldrich, 5.0 mL). The solutions were spin coated at 2000 rpm for 40 sec (E-flex, SC-4OP spin coater) on a cleaned FTO substrate (8 Ω, Pilkington). After spin-coating, the samples were pre-annealed onto a hot-plate at 300°C for drying. Spin coating and drying was repeated two more times. Finally, the films were annealed at 350, 450, and 550°C for 1 h in air to form the MnO_x electrocatalytic films onto the FTO substrate to be used as electrodes.

Electrochemical measurements.—The electrochemical properties of the MnO_x electrocatalytic films were investigated by using a potentiostat (Ivium, Iviumtechnology). The active area of the electrode was 0.5 cm². All measurements were carried out in 1 M NaOH (≥98%, Aldrich) electrolyte (pH = 13.7) at a scan rate of 10.0 mV/s. A platinum counter electrode and a Hg/HgO reference electrode in

⁼These authors contributed equally to this work.

^zE-mail: bkmin@kist.re.kr

1 M NaOH were used in a three-electrode configuration to characterize the catalytic activities for OER. All potential values were converted in terms of reversible hydrogen electrode (RHE) using $E(\text{vs. RHE}) = E(\text{vs. Hg/HgO}) + 0.140 + 0.059 \text{ V} \times \text{pH}$. Solution resistance (R_s) and charge transfer resistance (R_{ct}) were measured by circle fitting from electrochemical impedance spectroscopy (EIS) measurement by applying an AC voltage with 10 mV amplitude in a frequency range from 0.1 to 10 kHz. Potential values were compensated for iR loss and our electrochemical cell had $R_s = \sim 20 \Omega$ in 1 M NaOH. Electrochemical surface area (ECSA) was obtained by measuring the double-layer capacitance (C_{dl}) in a non-faradaic potential region from 0.20 to 0.25 V vs. Hg/HgO. The current density was measured at 0.245 V vs. Hg/HgO and plotted as a function of scan rate. The C_{dl} values were calculated from the slope of the current vs. the scan rate.

Characterizations.—Thermogravimetric analyses were carried out in air (TGA Q50, Netzsch, TG-209-type). The surface morphologies were imaged by field emission gun scanning electron microscopy (FEG-SEM, FEI Inc., Inspect F), and grazing incidence X-ray diffraction (GI-XRD, Rigaku corporation, D/Max 2500) with Cu-K α radiation (0.15406 nm) were used to characterize the crystal structure of the MnO $_x$ electrocatalytic films. Transmission electron microscopy (TEM, FEI, Tecnai) was used to characterize the crystal structure of MnO $_x$ films. X-ray photoelectron spectroscopy (XPS, VG Scientific, Sigma probe) with monochromated aluminum K α radiation was conducted to analyze the elemental composition. The C1s core level at 284.6 eV was used as a peak reference.

Results and Discussion

The MnO $_x$ electrocatalytic films were synthesized by using a simple annealing process in air after depositing Mn precursor solution on the FTO substrate. The annealing process has two main purposes of removing the ethylcellulose mixed in as a soft template and obtaining crystalline MnO $_x$ electrocatalytic films. Thus, the annealing temperatures were chosen to satisfy the complete removal of ethylcellulose where any residual polymer can restrict the OER activity while maintaining the integrity of FTO. In order to investigate the thermal decomposition process of the Mn precursor solution, a thermogravimetric (TG) analysis was carried out (Figure 1). A large weight loss

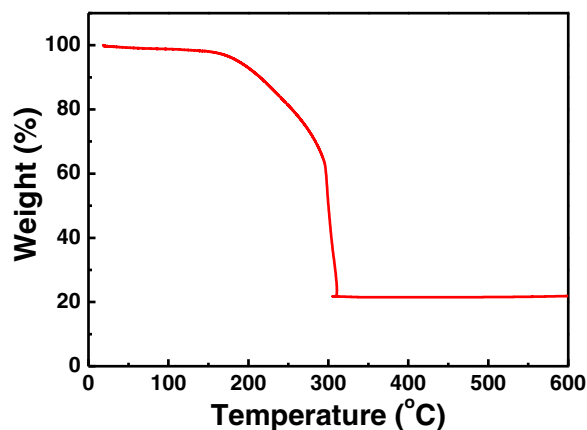


Figure 1. Thermogravimetric analyses (TGA) data of the Mn precursor solution for investigating the thermal decomposition.

was observed in the range between 200 and 300°C, which is attributed to elimination of ethylcellulose and terpineol. Also, we could confirm that there was no change in the weight when the temperature elevates higher than 325°C, which means the precursor has completely converted to crystalline MnO $_x$. Based on TG analysis, the preparation of MnO $_x$ electrocatalytic films were prepared at temperatures of 350, 450, and 550°C (below the FTO decomposition temperature, i.e. $\sim 600^\circ\text{C}$).

The surface morphology of each film was observed by SEM images (Figure 2). All films showed uniformly distributed nanoparticles having nanometer-sized pores, which was predicted previous experiments having ethylcellulose a soft template role.¹⁶ When comparing MnO $_x$ films prepared at 350 and 450°C, there was no change of particle sizes (~ 20 nm). However, we could confirm that the particle size of MnO $_x$ films prepared at 550°C was larger. Also, all films were uniformly deposited on the FTO substrate over the whole area and the thicknesses were estimated to be ~ 250 nm. As shown in Figure 3, XRD peak of the film prepared at 550°C was mainly assigned the formation of a spinel Mn $_2$ O $_3$ phase (JCPDS No. 41-1442). However, the film prepared at 350°C showed a different 2θ peak at 36.2°, corresponding

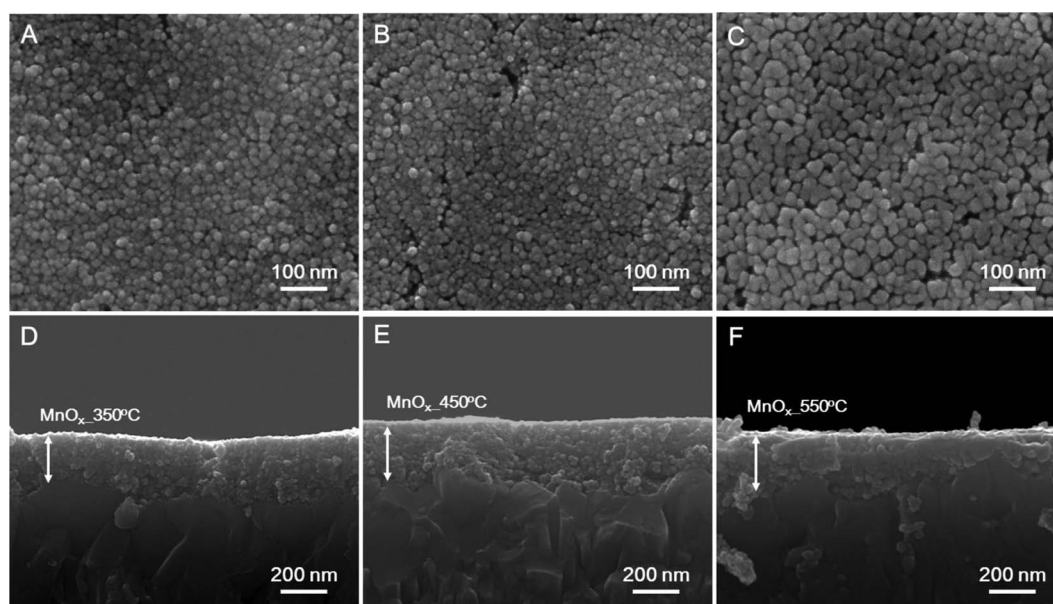


Figure 2. (A-C) Top view and (D-F) cross sectional SEM images of MnO $_x$ electrocatalytic films prepared at (A, D) 350, (B, E) 450, (C, F) 550°C.

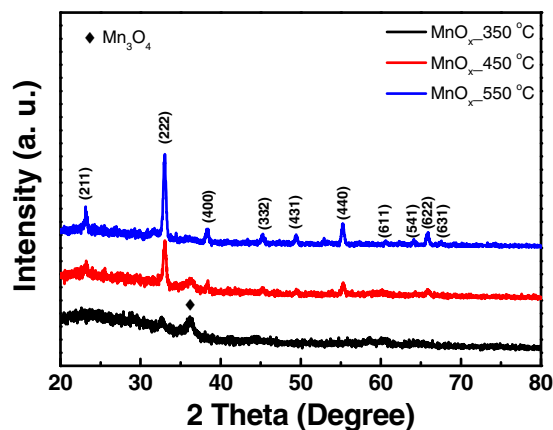


Figure 3. XRD patterns for MnO_x prepared at different temperature at 350, 450, and 550°C.

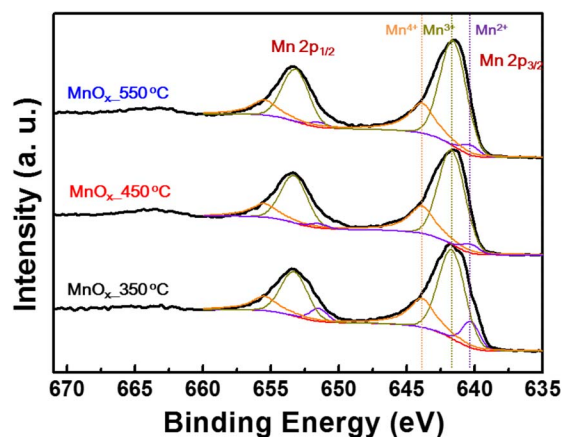


Figure 5. XPS spectra of MnO_x prepared at different temperature at 350, 450, and 550°C with narrow scan of Mn2p.

to the (211) plane of Mn_3O_4 (JCPDS No. 24-0734). Also, the film prepared at 450°C has both Mn_2O_3 and Mn_3O_4 phases. This result indicated that two different phase transition occurs from Mn_3O_4 to Mn_2O_3 in as the annealing temperature increases. In order to further confirm the crystallographic characteristics, a high resolution TEM images were obtained for all samples prepared at different temperatures (Figure 4). The lattice fringe for MnO_x prepared at 350°C show a clear spacing of 0.27 nm, which agrees well with the d_{211} spacing of Mn_2O_3 . On the other hand, those obtained at 450 and 550°C show a d_{211} spacing of 0.38 nm attributed to Mn_3O_4 . Thus the TEM results agree well with the results from XRD.

In order to confirm the chemical composition of the each electrocatalytic film, XPS analysis was performed. As shown in the Figure 5, XPS revealed the presence of the element Mn in the all electrocatalytic films. In the Mn2p region, the main peaks at 641.4 and 653.4 eV can each be assigned to $\text{Mn}2p_{3/2}$ and $\text{Mn}2p_{1/2}$ binding energies (BE).²⁰ As expected, when the $\text{Mn}2p_{3/2}$ peak was deconvoluted, we could confirm the presence of Mn^{2+} that may be attributed to the Mn_3O_4 phase but an excess amount of Mn^{3+} state was also found to be present. Solely from XRD, crystalline Mn_3O_4 a $\text{Mn}^{3+}/\text{Mn}^{2+}$ is expected to be 2; however, we assume that an amorphous Mn_2O_3 phase exists in the film prepared at 350°C because the ratio of $\text{Mn}^{3+}/\text{Mn}^{2+}$ species is significantly large (>5). Furthermore, we could confirm that the ratio of $\text{Mn}^{3+}/\text{Mn}^{2+}$ of the film prepared at 450 and 550°C was both over 15 that seems to be mainly present Mn^{3+} state in the Mn_2O_3 phase.

In order to confirm the OER activities of the three different electrocatalytic film, LSV measurement was conducted (Figure 6A). The overpotentials were determined at 426, 387, and 407 mV vs. RHE at

10 mA/cm² for MnO_x prepared at 350, 450, and 550°C, respectively. These results indicate that MnO_x prepared at 450°C showed the best performance for OER and the value of 387 mV at 10 mA/cm² was comparable to that of the best Mn-based OER catalysts synthesized with using various methods previously reported (Table I). When testing the stability of MnO_x electrocatalytic film prepared at 450°C at the 0.8 V vs. Hg/HgO, the current density slowly decrease from 10.3 to 8.0 mA/cm² after 5 h (Figure 6B). The deactivation of the OER activity for MnO_x electrocatalytic film may be affected by several factors such as corrosion, materials degradation, and surface passivation, etc.²¹ When the Tafel slope was calculated from LSV data, the value of MnO_x electrocatalytic film prepared at 350°C is ~ 80 mV while MnO_x prepared at 450 and 550°C shows lower Tafel slope, ~ 70 mV (Figure 6C). This result indicates that MnO_x prepared at 450 and 550°C shows a beneficial effect in accelerating OER kinetics than MnO_x prepared at 350°C. One possibility of different OER activities is the change of surface area in accordance with annealing temperature. Thus, the electrochemical surface area (ECSA) of the each electrocatalytic film was measured by double layer capacitance to verify this point (Figure 7).^{19,22} The electrochemical surface areas were 4.01, 2.12, and 1.01 mF/cm² for MnO_x electrocatalytic films prepared at 350, 450, and 550°C, respectively. Considering ECSA with the current density at 1.6 V vs. RHE, it was found that MnO_x electrocatalytic film prepared at 450°C had almost two times higher current density (5.99 mA/cm²) than that for MnO_x electrocatalytic film prepared at 550°C (3.09 mA/cm²), which is in good agreement with ECSA data of MnO_x electrocatalytic film prepared at 450 and 550°C. However, interestingly, MnO_x electrocatalytic film prepared

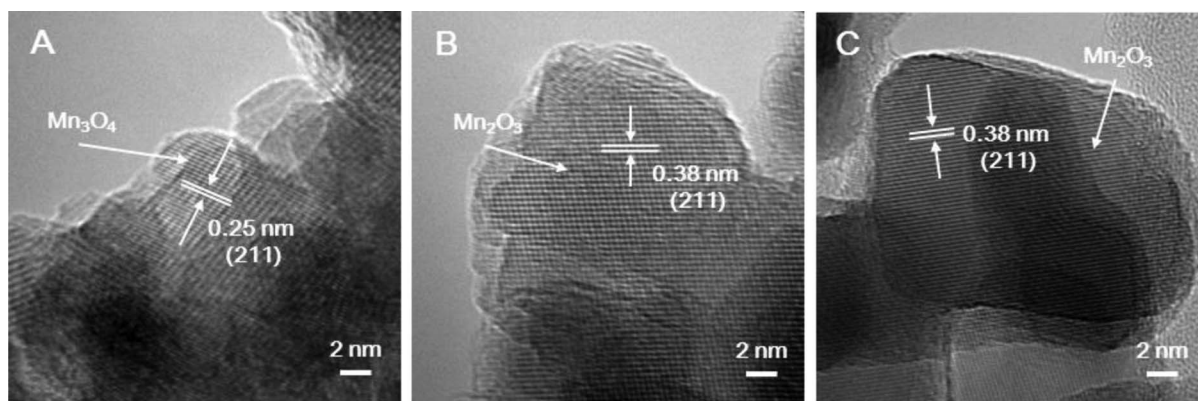


Figure 4. TEM images for MnO_x prepared at different temperatures at (A) 350, (B) 450, and (C) 550°C.

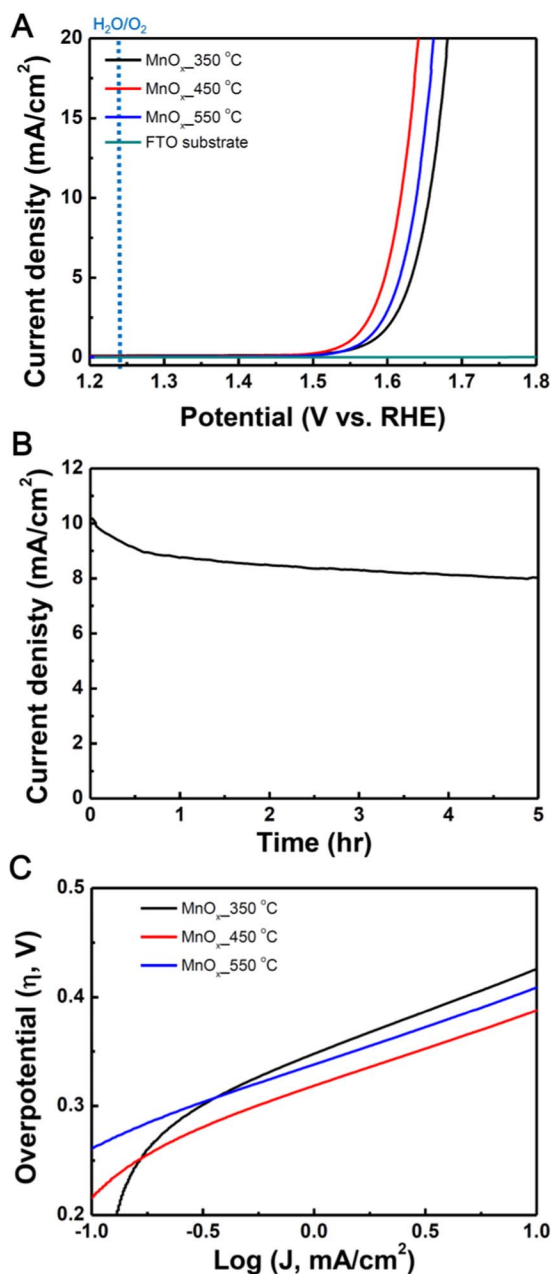


Figure 6. (A) LSV measurements of the MnO_x electrocatalytic films prepared at different temperature at 350, 450, and 550 °C, (B) The stability test at 0.8 V vs. Hg/HgO for 5 hr, and (C) Tafel slope of the MnO_x electrocatalytic films prepared at different temperature at 350, 450, and 550 °C.

at 350 °C had the lowest current density in spite of the highest surface area among the all electrocatalytic films. This result implies that additional factors play important roles in enhancing OER activity of the MnO_x electrocatalytic film prepared at 450 °C.

The change of OER activities for MnO_x electrocatalytic films depending on annealing temperature may be affected by several factors. In general, Mn³⁺ state in MnO_x catalysts is known to be the active site in OER.¹⁴ As mentioned above, we could confirm that MnO_x electrocatalytic film prepared at 350 °C is in the Mn₃O₄ phase that contains Mn²⁺ state on the catalyst surface. Thus, the number of active sites on the catalysts surface may be lower than the other films due to the relatively lower concentration of Mn³⁺ state. We could expect that enhanced activity for OER could be derived from the change of chemical composition of catalytic surface in accordance with temperature variation. To elaborate the phenomenon, when the charge transfer resistance (*R*_{ct}) was measured by electrochemical impedance spectroscopy (EIS), the value of MnO_x electrocatalytic film prepared at 450 °C (13.0 Ω) is 2.5 times lower than that of MnO_x prepared at 350 °C (32.7 Ω) (Figure 8). This result indicates that charge flow between electrocatalytic film and electrolyte have a faster electron transfer rate that can be facilitated for OER. The data of the electrochemical properties are summarized in Table I.

When comparing the OER activities of Mn-based OER catalysts synthesized with using various method, our results show the good performance with low overpotential at 10 mA/cm² (Table II). In general, to prepare catalytic films of MnO_x, binder materials such as Nafion and polyvinylidene fluoride (PVDF) are used to deposit the catalysts onto the conducting substrate after synthesizing MnO_x catalysts.^{13,14} These binder materials could adversely affect the OER catalytic activity by restricting contact between the catalyst and the electrocatalytic film.^{23,24} On the other hand, our MnO_x electrocatalytic films were directly deposited onto substrates with no binder material unnecessarily contributing the resistance in electron transfer. Furthermore, the distribution of nanoporous MnO_x electrocatalytic films on the substrate caused by ethylcellulose could facilitate the interactions between hydroxyl ions and active sites to generate oxygen by enhancing the inherent catalytic properties.¹⁶ Therefore, we suggest that a technique to exploit the inherent catalytic property of MnO_x has to be accompanied by the synergistic effects of an unimpeded catalysts surface without high resistive materials (e.g. Nafion) that is well distributed throughout the substrate. CSD is a suitable method to accomplish this aspect of electrocatalytic film processing.

Conclusions

Low cost processing of earth abundant materials for OER is actively pursued by the scientific community. In response, this work has successfully demonstrated that MnO_x electrocatalytic films can be processed using the CSD method. The OER activity heavily depended on the annealing temperature. MnO_x films processed at 450 °C

Table I. Comparison of different Mn₂O₃ electrocatalysts for water oxidation reaction activities.

	Synthesis method	Electrolyte (pH)	η (mV at mA/cm ²)	Tafel slope (mV/dec)	Ref.
Mn ₂ O ₃ (at 450 °C)	chemical solution deposition	1 M NaOH (pH 13.7)	387 mV at 10 mA/cm ²	69.3	This work
Mn ₂ O ₃ (at 350 °C)	chemical solution deposition	1 M NaOH (pH 13.7)	426 mV at 10 mA/cm ²	80.3	This work
Mn ₂ O ₃ (at 550 °C)	chemical solution deposition	1 M NaOH (pH 13.7)	407 mV at 10 mA/cm ²	68.5	This work
Mn ₂ O ₃	hydrothermal oxidation	1 M NaOH	400 mV at 1 mA/cm ²	N/A	25
Mn ₂ O ₃	solution process	0.1 M KOH	500 mV at 1 mA/cm ²	N/A	14
α-Mn ₂ O ₃	electrochemical deposition	1 M KOH (pH 14)	360 mV at 10 mA/cm ²	N/A	26
Mn ₂ O ₃	electrochemical deposition	0.1 M KOH (pH 13)	750 mV at 8 mA/cm ²	N/A	19
Mesoporous-Mn ₂ O ₃	sol-gel process	Na ₂ SiF ₆ -NaHCO ₃ buffer solution (pH 5.8)	507 mV at 10 mA/cm ²	N/A	13
α-Mn ₂ O ₃	electrochemical deposition	1 M KOH	570 mV at 20 mA/cm ² , ~430 mV at 10 mA/cm ²	N/A	8

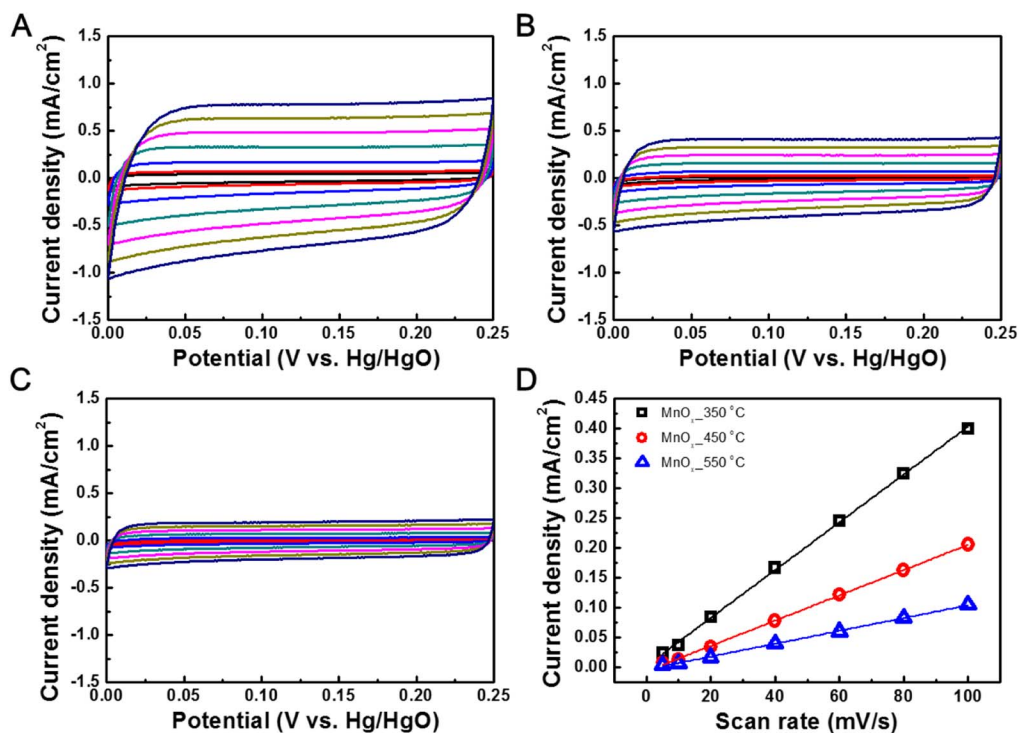


Figure 7. Cyclic voltammety measurements of MnO_x electrode prepared at (A) 350, (B) 450, and (C) 550°C. (D) Plot of the current density measured at 0.245 V vs. Hg/HgO plotted as a function of scan rate.

Table II. Summary of electrochemical properties of MnO_x electrocatalytic films prepared at different temperature at 350, 450, and 550°C.

	Overpotential (at 10 mA/cm ²)	Current density (at 1.6 V vs. RHE)	C _{dl} (ECSA)	R _{ct}	Tafel slope
MnO _x _350°C	426 mV	2.03 mA/cm ²	4.01 mF/cm ²	32.7 Ω	80.3
MnO _x _450°C	387 mV	5.99 mA/cm ²	2.12 mF/cm ²	13.0 Ω	69.3
MnO _x _550°C	407 mV	3.09 mA/cm ²	1.01 mF/cm ²	19.6 Ω	68.5

exhibited a greater electrochemical surface area, higher surface density of Mn³⁺ state, and lower charge transfer resistance resulting in an overpotential of 387 mV at 10 mA/cm². XRD analysis identified the presence of crystalline Mn₃O₄ and XPS deconvolution deduced an amorphous Mn₂O₃ due to the Mn³⁺/Mn²⁺ ratio exceeding that of Mn₃O₄. The comparable performance of the MnO_x films synthesized by CSD shows promise as one of the methods to be applied for the commercialization of electrochemical OER.

Acknowledgments

This work was supported by a grant of the National Research Foundation of Korea (University-Institute cooperation program) funded by the Ministry of Science, ICT, and Future Planning and partly by the internal program of Korea Institute of Science and Technology (KIST).

References

1. M. Gong, Y. Li, H. Wang, Y. Liang, J. Z. Wu, J. Zhou, J. Wang, T. Regier, F. Wei, and H. Dai, *J. Am. Chem. Soc.*, **135**, 8452 (2013).
2. A. Kudo and Y. Miseki, *Chem. Soc. Rev.*, **38**, 253 (2009).
3. M. G. Walter, E. L. Warren, J. R. McKone, S. W. Boettcher, Q. Mi, E. A. Santori, and N. S. Lewis, *Chem. Rev.*, **110**, 6446 (2010).
4. L.-K. Wu and J.-M. Hu, *Electrochim. Acta.*, **116**, 158 (2014).
5. H. S. Jeon, J. H. Koh, S. J. Park, M. S. Jee, D.-H. Ko, Y. J. Hwang, and B. K. Min, *J. Mater. Chem. A*, **3**, 5835 (2015).
6. T. Takashima, K. Hashimoto, and R. Nakamura, *J. Am. Chem. Soc.*, **134**, 1519 (2012).
7. M. M. Najafpour and M. M. Govindjee, *Dalton Trans.*, **40**, 9076 (2011).
8. H.-Y. Su, Y. Gorlin, I. C. Man, F. Calle-Vallejo, J. K. Nørskov, T. F. Jaramillo, and J. Rossmeisl, *Phys. Chem. Chem. Phys.*, **14**, 14010 (2012).
9. Y. Gorlin and T. F. Jaramillo, *J. Am. Chem. Soc.*, **132**, 13612 (2010).
10. K. L. Pickrahn, S. W. Park, Y. Gorlin, H.-B.-R. Lee, T. F. Jaramillo, and S. F. Bent, *Adv. Energy Mater.*, **2**, 1269 (2012).
11. A. Indra, P. W. Menezes, I. Zaharieva, E. Baktash, J. Pfrommer, M. Schwarze, H. Dau, and M. Driess, *Angew. Chem. Int. Ed.*, **52**, 13206 (2013).
12. K. L. Pickrahn, Y. Gorlin, L. C. Seitz, A. Garg, D. Nordlund, T. F. Jaramillo, and S. F. Bent, *Phys. Chem. Chem. Phys.*, **17**, 14003 (2015).
13. A. Singh, D. Roy Chowdhury, S. S. Amritphale, N. Chandra, and I. B. Singh, *RSC Advances*, **5**, 24200 (2015).

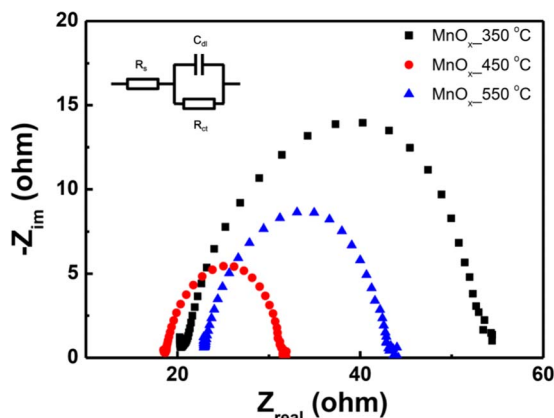


Figure 8. Electrochemical impedance spectroscopy (EIS) data of MnO_x electrode prepared at 350, 450, and 550°C. (Inserted figure is the equivalent circuit).

14. C.-H. Kuo, I. M. Mosa, A. S. Poyraz, S. Biswas, A. M. El-Sawy, W. Song, Z. Luo, S.-Y. Chen, J. F. Rusling, J. He, and S. L. Suib, *ACS Catal.*, **5**, 1693 (2015).
15. T. Schneller, Springer, Wien; New York, (2010).
16. H. S. Jeon, M. S. Jee, H. Kim, S. J. Ahn, Y. J. Hwang, and B. K. Min, *ACS Appl. Mater. Inter.*, **7**, 24550 (2015).
17. S. Ito, P. Chen, P. Comte, M. K. Nazeeruddin, P. Liska, P. Péchy, and M. Grätzel, *Prog. Photovoltaics*, **15**, 603 (2007).
18. S. J. Park, J. W. Cho, J. K. Lee, K. Shin, J.-H. Kim, and B. K. Min, *Prog. Photovoltaics*, **22**, 122 (2014).
19. A. Ramírez, P. Hillebrand, D. Stellmach, M. M. May, P. Bogdanoff, and S. Fiechter, *J Phys. Chem. C*, **118**, 14073 (2014).
20. G. Yang, W. Yan, J. Wang, and H. Yang, *CrystEngComm.*, **16**, 6907 (2014).
21. N. Li, W.-Y. Xia, J. Wang, Z.-L. Liu, Q.-Y. Li, S.-Z. Chen, C.-W. Xu, and X.-H. Lu, *J. Mater. Chem. A*, **3**, 21308 (2015).
22. C. C. L. McCrory, S. Jung, J. C. Peters, and T. F. Jaramillo, *J. Am. Chem. Soc.*, **135**, 16977 (2013).
23. C. Yuan, H. B. Wu, Y. Xie, and X. W. Lou, *Angew. Chem. Int. Ed.*, **53**, 1488 (2014).
24. M. Cabo, E. Pellicer, E. Rossinyol, M. Estrader, A. Lopez-Ortega, J. Nogues, O. Castell, S. Surinach, and M. D. Baro, *J. Mater. Chem.*, **20**, 7021 (2010).
25. P. Hillebrand, A. Ramirez-Caro, W. Calvet, P. Bogdanoff, and S. Fiechter, *ECS Transactions*, **61**, 9 (2014).
26. S. Y. Lee, D. González-Flores, J. Ohms, T. Trost, H. Dau, I. Zaharieva, and P. Kurz, *ChemSusChem*, **7**, 3442 (2014).